VSP

Advanced Robotics 23 (2009) 1131–1158

ADVANCED ROBOTICS
www.brill.nl/ar

Full paper

Parameterized and Scripted Gaits for Modular Snake Robots

Matthew Tesch, Kevin Lipkin, Isaac Brown, Ross Hatton, Aaron Peck, Justine Rembisz and Howie Choset *

Department of Robotics, Carnegie Mellon University, Pittsburgh, PA 15213, USA

Received 3 October 2008; accepted 17 February 2009

Abstract

Snake robots, sometimes called hyper-redundant mechanisms, can use their many degrees of freedom to achieve a variety of locomotive capabilities. These capabilities are ideally suited for disaster response because the snake robot can thread through tightly packed volumes, accessing locations that people and conventional machinery otherwise cannot. Snake robots also have the advantage of possessing a variety of locomotion capabilities that conventional robots do not. Just like their biological counterparts, snake robots achieve these locomotion capabilities using cyclic motions called gaits. These cyclic motions directly control the snake robot's internal degrees of freedom which, in turn, causes a net motion, say forward, lateral and rotational, for the snake robot. The gaits described in this paper fall into two categories: parameterized and scripted. The parameterized gaits, as their name suggests, can be described by a relative simple parameterized function, whereas the scripted cannot. This paper describes the functions we prescribed for gait generation and our experiences in making these robots operate in real experiments.

Keywords

Locomotion, hyper-redundant mechanism, snake robot, gait design, motion planning

1. Introduction

In recent years, a certain class of robots called snake robots have gained considerable attention because of their unique ability to locomote over a variety of terrains. These robots, also called hyper-redundant mechanisms, inherit their maneuverability from their unique shape-changing capabilities. Their long and slender shape, along with their many internal degrees of freedom (d.o.f.), allows them to thread through tightly packed volumes without disturbing surrounding areas. This shape also allows actuators to be distributed down the length of the device. Such a distribution enables a greater range of interaction between the environment

* To whom correspondence should be addressed. E-mail: choset@cs.cmu.edu

 DOI:10.1163/156855309X452566

and the mechanism, as compared to conventional wheeled devices and legged machines.

The snake robots' potential to locomote in a variety of terrains suggests a number of practical applications. In particular, we have been interested in applying snake robot technology to aid rescue workers in locating victims who may be trapped in a collapsed or bombed building where mobility is severely limited and the environment is difficult to evaluate. In this scenario, snake robots are well suited to extend the reach of rescue workers and speed the retrieval of trapped victims. With a camera and microphone deployed at the distal end of the robot and other sensors along its body, rescue workers may be able to use snake robots to more quickly locate survivors and diagnose problems. Further, the snake robot can bring sustenance to survivors and potentially transfer supplies for rescue workers.

Search and rescue, along with other safety, security and response applications, are thus facilitated by snake robot technology because of the many d.o.f. of these mechanisms. These many d.o.f., however, pose deep fundamental research questions, including but not limited to mechanism design and motion planning. In terms of mechanism design, we have already built a family of 16-d.o.f. snake robots [1, 2]. Our design is modular; each module consists of a standard hobby servo with electronics replaced to give the servos more power and to enable addressability. The electronics in each module include a microcontroller, H-bridge, switching power supply, magnetic encoder, current sensor and temperature sensor, all of which in turn perform low-level PID control, interfacing and safety checks. To produce motion in three dimensions, the axes of two adjacent modules are offset by 90°.

The primary contribution of this paper is not the robot itself, but rather the motion planning: determining the necessary inputs to the snake robot system to propel it in a desired direction. We address motion planning by designing gaits — cyclic motions of the internal variables of the robot that cause desired net displacements. Already, we have designed gaits to enable snake robots to crawl on the ground, sidewind like a real snake, climb a pole and swim in a pond, as shown in Fig. 1.

This paper describes two classes of gaits, categorized by whether or not they can be described by a parameterized function such as a sinusoid. Most biologically inspired gaits, such as lateral undulation, fall into the parameterized category, as do some non-biological gaits such as pole climbing. Varying the parameters on any of these gaits allows an operator to continuously alter the resulting motion. Other gaits, such as stair climbing, cannot be reasonably represented by a single parameterized function. These gaits, called scripted gaits, are implemented by stepping the snake robot through a series of predefined shapes.

After presenting the parameterized and scripted gaits, this paper looks at the energetics of these gaits, both on the macroscopic mechanism and the individual modules in the device. This has informed us on how to better define the gaits and will one day serve as useful information for feedback control. Finally, the paper concludes with experiments performed at the Southwest Research Institute and energetic measurements of gaits which were evaluated.

Figure 1. Our locomoting robots: reaching across a gap (top left), traversing through brush (top right), climbing the inside of a clear pipe (bottom left) and swimming (bottom right).

2. Carnegie Mellon Modular Snake Robots

Our snake robots contain a series of single-d.o.f. revolute joints connected in a chain where each axis of rotation is offset by 90° such that half of the joints actuate in the vertical plane and the other half in the horizontal plane; this geometry allows for motion in three dimensions. For clarification, refer to Fig. 2, which shows a basic schematic of the mechanism. Figure 3 shows some of the snake robots that we have built over the past several years; the geometry of these mechanisms has remained relatively constant. We currently exclusively use the most recent generation of the robots. Typically our snake robots have 16 modules, but this number can vary for special applications. A 16-module snake robot of the latest design is shown in Fig. 4; this snake has length 97 cm, diameter 5.3 cm and weight 1.8 kg.

Each module of the snake robot contains a single actuator. On some previous designs, these actuators were simply hobby servos and the robot had many wires running throughout the snake in order for a centralized computer to control each module individually. However, in our more recent snake robots, we have redesigned the electronics of each servo, allowing all control and communication to occur on a two-wire serial bus. This reduces the number of wires running through the snake robot to a total of only six: two for control of and communication with the modules,

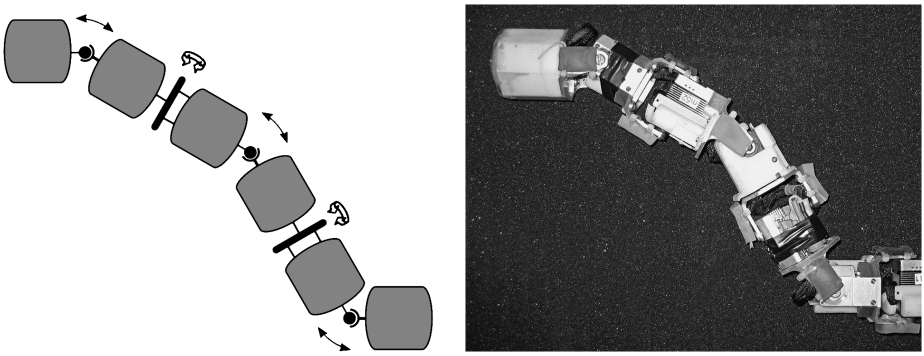

Figure 2. Basic schematic of the snake robot design. Each joint axis is orthogonal to its neighbors and has a range of $\pm 90^\circ$. Although these images only show six modules, we typically configure a snake with 16 modules.

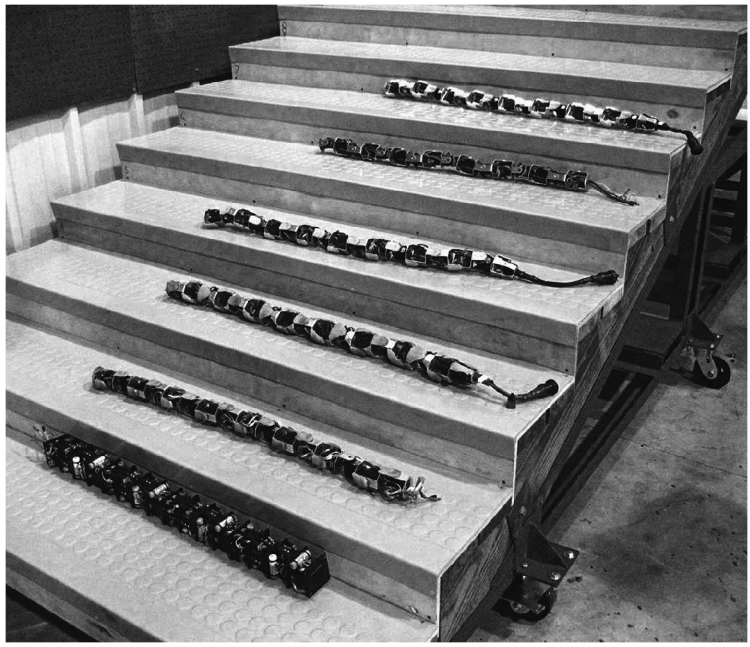

Figure 3. A few of our snake robots. From the bottom to the top (old to new), the robots are named Meatloaf, Chip, Hercules, Sir Hiss, Khan and Elizabeth.

two for video from the camera and two for power. This reduction in wire count decreases the likelihood of failure. Additionally, the new electronics allow each motor to deliver more torque and provide the controller with state information from the module, such as current, temperature and position.

As with almost all of our snake robots, the current state-of-the-art robots utilize a tether, primarily for power. Naturally, we seek to include onboard power, but our current efforts focus on gait generation as opposed to mechanism and electronics

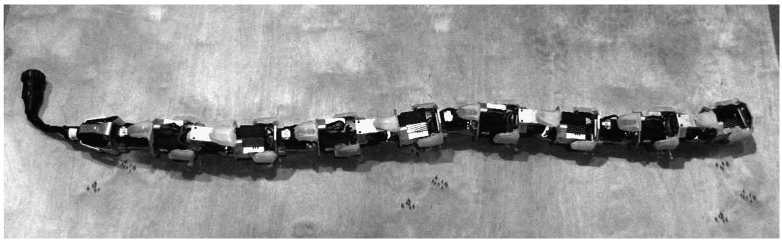

Figure 4. Elizabeth, a robot of the latest design, shown here in the typical 16-module configuration.

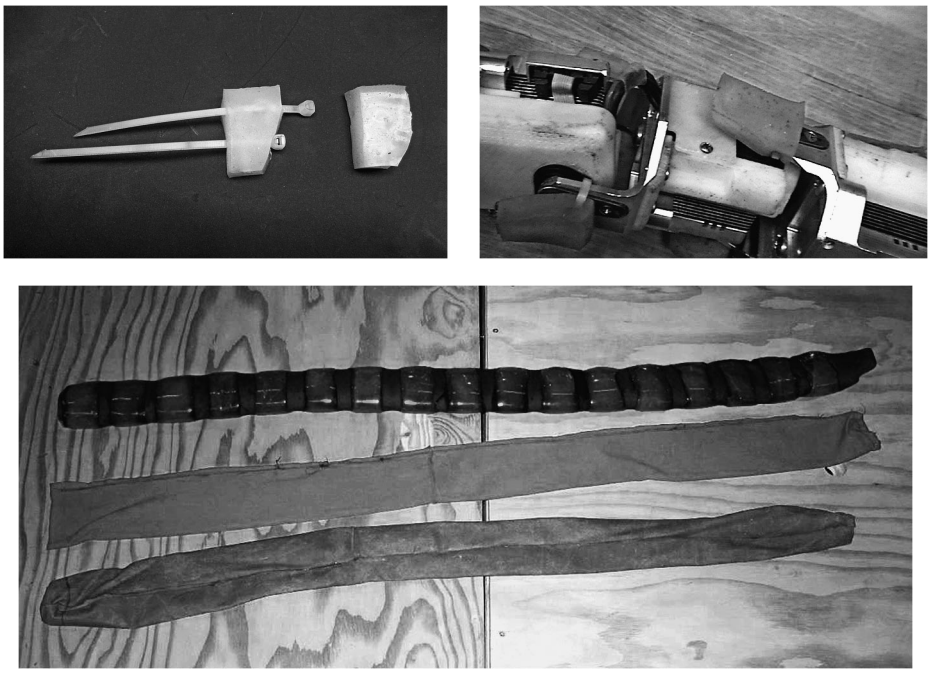

Figure 5. Platinum-doped silicon patches of Dragon Skin™ mounted on each module (top) and skins that encase the entire robot (bottom).

development. However, it is worth pointing out that some applications, including urban search and rescue as well as mine rescue, require a tether for safety and retrieval purposes.

Our snakes feature two types of skin: one consisting of individual patches of compliant material and the other fully encasing the robot. The first type, shown in Fig. 5, is composed of patches of Dragon Skin™. This material is platinum-doped silicone, which provides compliance between the robot and the terrain. These compliant patches reduce shock loads and extend contact areas, while increasing the diameter of the robots to 6.4 cm. These patches are also critical for locomotion using our gaits, as the additional friction allows the snakes to more effectively push against the surfaces they locomote across. Figure 5 additionally shows the second

type of skin, which encases the robot and is more appropriate for travel through sand and brush, to prevent entrainment of particles and debris. This type of skin is made of commercially available fabric and sewn to accommodate the cylindrically shaped robots.

3. Related Work

During the course of evolution, biological snakes are believed to have lost their limbs to move effectively in cluttered and highly convoluted terrestrial environments, such as underground chasms and in and between cracks and crevices [3]. However, when snake lineages returned to the surface with open terrains, they acquired new, adaptive modes of locomotion without need for redevelopment of legs or *de novo* evolution of other leg-like structures. Inspired by the success of snakes in virtually every domain on the planet, a certain class of robots called snake robots has gained considerable attention by the robotics community. Formally called hyper-redundant mechanisms [4, 5], snake robots inherit their maneuverability from their unique shape-changing capabilities.

3.1. Biological Snake Gaits and Energetics

It goes without saying that the gait work in this paper takes profound inspiration from biology. Although this work is not strictly copying biology, understanding the four fundamental motions of biological snakes provides an excellent starting point for our modeling. The four main modes are:

- *Lateral undulation*. Fish move forward by shaping their bodies in an 'S-shaped' curve that travels tailwards [6, 7]. Almost all limbless vertebrates, including snakes, mimic their ancestors by using this kind of locomotion for traversing the ground. Snakes propel themselves on the ground by summing the longitudinal resultants of posterolateral forces. Biologists do not agree on the energetic cost of snakes using lateral undulation. Chodrow and Taylor claim that lateral undulation requires half the metabolic cost compared to tetrapods of equivalent mass [8], while Walton *et al*. claim that energetic cost is comparable between undulating snakes and locomoting tetrapods of the same size and mass [9].
- *Concertina*. When a snake is placed in narrow surroundings, it instinctively 'elbows out' regions of its body to establish static points of contact. Using the static points as fixtures, the body moves forward by pushing on the environment, seemingly moving the static points backwards. Due to the stop-and-go movement of the body of the snake, momentum is not conserved and, thus, the mode of motion is energetically expensive and slow. Walton *et al*. claim that concertina is 7 times less efficient when compared to other kinds of locomotion in real snakes [9]. Snakes use concertina only when other options of locomotion are ineffective, such as while traversing tight spaces with high friction.

- *Linear progression*. In this mode of locomotion, the snake anchors its body at certain sites that seem to continuously move tailwards. Inchworms exhibit this motion with one very large wave, whereas biological snakes use numerous minuscule waves. For snakes, some critical aspects of this kind of locomotion are that the snake ribs operate in parallel, the skin must possess appreciable anteroposterior flexibility and most of the snake's mass moves forward at a constant speed. Linear progression is energy efficient due to conservation of momentum.
- *Sidewinding*. Snakes generally use this gait to locomote on sand and loose gravely substrate. At any given instant, at least two portions of the snake are in static contact with the ground. The rest of the snake body is lifted and moves forward. The snake uses small irregularities in the surface against which it pushes sideways. Sidewinding conserves momentum and is claimed to be the most efficient mode of snake locomotion [10].

3.2. Prior Snake Robot Modeling

There are three chief classes of hyper-redundant robots: elephant trunks, direct-drive snakes and true snakes. Elephant trunk robots are either mounted on a fixed base [11, 12], or a mobile base [13, 14] to increase their reach. Direct-drive snake robots derive their propulsion from a moving tread or skin [15, 16]. Finally, true snake robots derive their propulsion from internal shape changes [17–19].

Drawing inspiration from biology, Hirose, with his 1972 pioneering work in snake robots, implemented lateral undulation on simple planar snake robots [17]. Miller, Ostrowski, and others have been experimenting with this kind of locomotion as well [18, 20]. All of these efforts use passive wheels under the robot body. These passive wheels theoretically provide infinite and null friction in the lateral and the axial direction, respectively, which is essential in propelling the snake robot forward. Ultimately, all of these methods propel the robot on very flat terrains and use more energy than a conventional wheeled robot of comparable size.

Another method of modeling gaits is demonstrated in Chirikjian and Burdick's [5] backbone approach, where the mechanism is fit to a one-dimensional (1-D) curve embedded in a 3-D space. The question then becomes: what is this backbone curve? Intuition would suggest that backbone curves for real snakes are sinusoids. However, Hirose showed that for lateral undulation these curves are actually the serpenoid curve, which has a sinusoidal curvature [21].

Further work has been done on modeling biological snake gaits besides lateral undulation. Chirikjian and Burdick implemented linear progression on their planar snake robot and Yim also implemented linear progression on his modular polybots [22]. Other research into robotic snake gaits includes Chirikjian and Burdick's basic research on sidewinding [4], and Barazandeh *et al.*'s examination of concertina locomotion [23]. Gonzalez-Gomez *et al*. have demonstrated a model for various gaits that is perhaps the most similar to that presented here; however, their model is

based on a set of coupled functions individually describing the angle for each joint, rather than a single function for the entire mechanism [24, 25].

3.3. Prior Snake Robot Mechanism

Our design bears a strong similarity to Yim's Polypods [22] and Shen's Superbot [26], which is no surprise because our snake robots have a modular design inspired by Yim's work. Moreover, both Yim and Shen have demonstrated some snake robot gait capability. However, Yim's and Shen's works do not focus on snake robot gaits, but rather on modularity and reconfiguration. They are not designing sophisticated, efficient gaits but rather assume a pre-existing library of modes of locomotion and then search different graph topologies of the various configurations to achieve a particular locomotion capability. We, on the other hand, are developing locomotion capabilities for snake robots through algorithmic prescription and efficient experimentation. In other words, they fix a locomotion mode and search for a configuration; we take a configuration and find the best locomotion mode. One could imagine an iterative process that goes back and forth between the two, making these methods complementary.

4. Modeling

Drawing from our experimental experiences, we address the challenge of designing gaits by searching for a model that allows us to describe the inputs to the snake robots. For our robots, these inputs are desired joint angles, as we have a single actuated d.o.f. at each joint. Since snake gaits are in general cyclic, intuitive choices of functions for describing joint motions might include the sinusoids that generate Hirose's serpenoid curve [21].

In fact, this intuition of using sinusoids is the basis for all of the basic gaits we have formed, which fall into a class of gaits called parameterized gaits — named as such because they can be described by a parameterized function. Many times a task may require a more complicated set of motions that one parameterized gait cannot provide. For example, our current version of stair-climbing requires the robot to undergo a sequence of distinct motions: move along the step, reach up and over, coil, and repeat. Here, we have distinct motion segments, which when patched together form a stair-climbing gait. We describe these types of complex gaits as scripted because the intermediate configurations of the gait follow a set of predefined waypoints in configuration space.

4.1. Parameterized Gaits

Parameterized gaits are beneficial since they can be described by relatively simple functions. All of our parameterized gaits are based upon sinusoidal waves lying in two mutually perpendicular planes: a horizontal plane parallel to the ground, and a vertical plane perpendicular to the ground and parallel to the longitudinal axis of the snake. Recall that the actual mechanism consists of orthogonally placed, single rotational d.o.f. joints, where we ascribe the even joints to modules that bend

in the vertical plane and odd joints to modules that bend in the horizontal plane (Fig. 2). So, if a vertical wave perpendicular to the ground is sent through the mechanism, only the even modules participate, while the odd modules remain stationary. Likewise, only the odd modules participate in sending lateral waves parallel to the ground through the robot. Should the snake robot fall onto its side, then the even modules simply become the lateral modules and the odd become the vertical modules.

Ultimately, the joint angles describe the gait. For the parameterized gaits we present here, each joint angle is modeled as a sine function with an offset. The angle of the nth module at time t, given by $\alpha(n, t)$, is:

$$\alpha(n,t) = \begin{cases} \beta_{\text{even}} + A_{\text{even}} \sin(\theta), n = \text{even}, \\ \beta_{\text{odd}} + A_{\text{odd}} \sin(\theta + \delta), n = \text{odd}, \end{cases} \tag{1}$$

$$\theta = \left(\frac{\mathrm{d}\theta}{\mathrm{d}n} n + \frac{\mathrm{d}\theta}{\mathrm{d}t} t \right), \tag{2}$$

where β, A, θ and δ are, respectively, offset, amplitude, frequency and phase shift terms illustrated in Fig. 6, and described in more detail below. All of these parameters can be modified to change both the type and nature of the gait performed by the robot. Effectively, this equation states that the joint angles along the snake change as a sine wave, both with respect to module number and with respect to time.

These equations specify the curvature of the backbone curve at discrete intervals, as opposed to directly specifying this curve. The frequency of this wave, which specifies the joint angles, is determined by θ. Note that this is the same as the

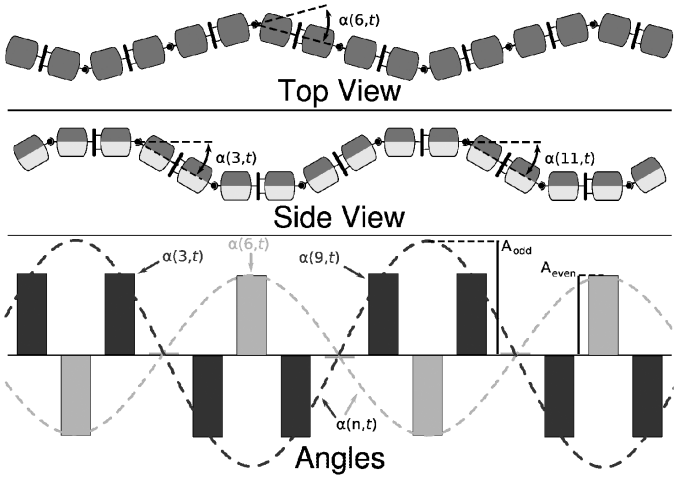

Figure 6. Snake robot (with modules that are shaded on top to aid visualization) shown from a top view and side view, along with a graph that shows $\alpha(n, t)$ for each module. Superimposed on this graph are dotted lines representing the continuous sine wave that these angles α are generated from. Note that since these are discrete samples from a continuous wave, at a given time t there may be no module at the peak of the wave.

frequency of the backbone curve of the snake, since these two equations are related *via* a second derivative operation.

The sine wave moving through the robot has both a spatial and temporal frequency component. First, $\frac{d\theta}{dn}$ determines the spatial component, meaning that if we fix t, $\frac{d\theta}{dn}$ describes the macroscopic shape of the robot. Another way of visualizing this parameter is that it is related to the wavelength along the robot; in the case of Fig. 6, this wavelength is four modules, so the spatial frequency is $2\pi/4$. Second, $\frac{d\theta}{dt}$ determines the frequency of the temporal component, meaning that if we examine the trajectory of one individual actuator (fix n), we determine how quickly the actuator cycles. Roughly, this indicates the speed of the wave. A zero value for $\frac{d\theta}{dn}$ causes identical angles on all of the modules on one axis, generating an arc (or possibly a straight line) along that axis, and a zero value for $\frac{d\theta}{dt}$ has the effect of freezing time.

The δ term is simply a phase shift to control the timing between the motions of the two orthogonal waves. In Fig. 6, since there is a half cycle between the green even module wave and the blue odd module wave, δ would be π.

Finally, the offsets, given by the β terms, are generally used to steer the robot when locomoting on the ground, as shown in Fig. 7. For instance, when the snake robot is moving in a straight line or climbing a pipe, the offsets are zero. The amplitude terms, A_{even} and A_{odd}, describe the amplitudes of the mutually perpendicular waves. In most cases, the amplitude and velocity of the robot are directly correlated, and as both increase, the robot can better reach over large obstacles. However, larger amplitude comes at the cost of reduced stability.

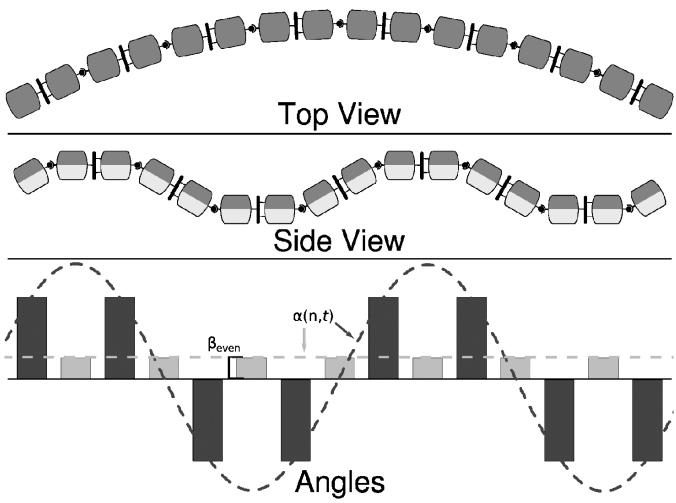

Figure 7. Parameter β_{even} describes the offset of half of the modules in the snake (using the same shading scheme as Fig. 6). Here, we see that a constant offset causes the modules to form an arc. Although in this example there is no sine wave on the even axis, a non-zero amplitude wave could be superimposed on this axis.

4.1.1. Biologically Inspired Parameterized Gaits

We make no claims on the generality of the model in (1) and (2). However, by appropriately varying the parameters we can achieve locomotive gaits that resemble linear progression, lateral undulation, sidewinding and other biological gaits. Linear progression, pictured in Fig. 8, is achieved by setting the amplitude of the lateral wave to zero and running a purely vertical wave through the snake. Loosely speaking, modules are picked up from the rear of the robot, brought forward through the air and placed upon the ground again as the waves progress.

While executing linear progression, the waves cause the robot's center of gravity to rise. This, combined with the fact that the robot's footprint is simply a straight line, may cause the robot to tip over laterally. To stabilize the robot, we position the lateral modules to widen the robot's footprint. The simplest way to perform this stabilization is to set the offset associated with lateral modules to a non-zero value, causing the lateral modules to form a stable arc while the vertical modules continue to propel the robot with waves. This arc shape has the additional benefit of allowing the operator to steer the robot by changing the radius and direction of the arc. An alternative stable footprint which still allows perfectly straight motion is an 'S' shape, which is generated in the lateral axis with two opposite arcs in the front and back half of the snake robot.

To achieve linear progression around corners in situations where there is not enough room to use a smooth arc, such as inside pipes, we create a sharp bend in the robot on the lateral axis that conforms to the corner. To continue conforming to the corner while the robot moves forward, the bend is moved backwards relative to the robot. The bend must be transitioned gradually from the n to the $n + 2$ (next lateral) module, synchronized with the progress of the robot such that the total bend angle remains contoured to the corner.

Originally, we intended to use a form of concertina locomotion to achieve climbing in a vertical channel, but found a variant linear progression to more readily enable the robots to climb vertical channels. The amplitude of the wave must be

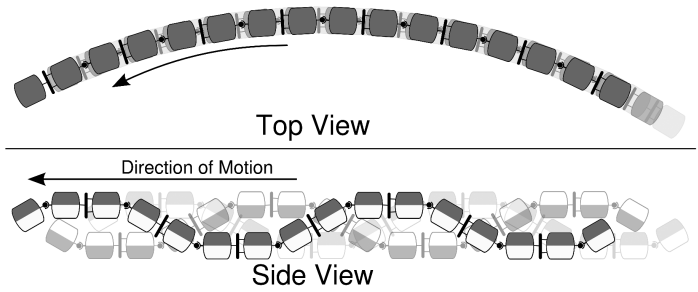

Figure 8. In linear progression, a wave is sent through the vertical modules, which serves to repeatedly pick up modules, bring them forward through the air and place them slightly forward of their starting position on the ground. The lateral modules are used purely for steering and balance of the robot. In this and future figures, to visualize the motion of the snake over time, we show multiple snapshots of the robot, which fade as their age increases.

large enough that the robot pushes outwards against the walls. This climbing gait surpasses concertina locomotions since (i) momentum is conserved as waves move forward through the robot and (ii) concertina locomotions tend to focus joint load over only a few modules. If the channel is sufficiently deep, the robot can be steered in and out of the channel using a lateral arc, the same way it can be steered left and right on the ground.

Linear progression can also be used to climb the inside of pipes, similar to how the robot climbs channels. However, since pipes, unlike channels, are fully enclosed, linear progression can be enhanced specifically for pipe climbing. With δ set to zero, and with equal amplitudes for both the vertical and lateral modules, there will be identical vertical and lateral sinusoids along the snake. The superposition of these two waves will cause the physical shape of the robot to follow a sine wave along a diagonal between the vertical and lateral plane. This 'double linear progression' allows all 16 modules to participate in the wave, as opposed to only the eight 'vertical' modules typically used to propel the robot. With double linear progression, the robot is able to climb wider pipes than is possible with single linear progression and is also able to climb more quickly.

Whereas linear progression largely deals with modules in the vertical plane, lateral undulation (Fig. 9) involves modules in the horizontal plane. This is achieved by setting the even amplitude to zero and the odd amplitude to a non-zero value. We demonstrated lateral undulation on our snake robots swimming in the water. In order to swim, we place the snakes in a waterproof skin.

Sidewinding is another biological gait that has inspired our robot gaits. Identical vertical and lateral waves with $\delta = \frac{\pi}{4}$ are used to perform sidewinding. Setting $\delta = \frac{\pi}{4}$ causes the robot to move almost directly sideways because the lateral wave begins to translate modules to the side just as they are at the peak of the vertical wave, where the modules are free from friction with the ground. The modules are then set back down by the vertical wave just before the lateral wave returns to the initial position. However, now that they are on the ground, the lateral modules are restricted by friction. The fact that the modules experience friction when moved in one direction, but not the other, leads to a net force from the ground to the robot in the desired direction. In this manner, the snake locomotes sideways, orthogonally to its length. By modifying the value of δ, the angle at which the snake robot

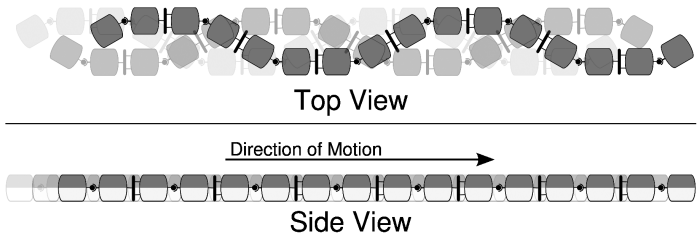

Figure 9. In lateral undulation, a wave is sent through the horizontal modules. This gait is often used for swimming.

moves sideways can be controlled. This is useful to achieve motion along a diagonal.

As with linear progression, the amplitude controls how aggressively the gait is performed, while $\frac{d\theta}{dn}$ controls the number of waves in the robot. Sidewinding's inherent stability due to its wide footprint allows the gait to be run with large amplitudes, allowing rapid progression and traversal over obstacles. Having the front and back halves of the robot perform sidewinding, but in opposite directions, produces an alternative use for the sidewinding gait. The resulting motion is that the snake robot rotates in place about its center.

Another hybrid of linear progression and lateral undulation is a gait called slithering, which is produced by having the lateral axis execute a sine wave with half of the frequency of the vertical wave. This additional frequency parameter requires a slight modification of our model. The slithering gait can be conceptualized as simple linear progression, except the lateral wave is continually undulating the snake robot. Visually, slithering resembles lateral undulation in that the lateral wave is larger and more prominent than the vertical wave.

4.1.2. Non-biologically Inspired Parameterized Gaits

We have also designed a number of gaits not inspired by biological snakes. Our inspiration for developing these gaits was to achieve specific tasks quickly and reliably. One such gait is rolling, where the robot forms a smooth arc and then rolls side over side across the ground. To achieve this motion, $\frac{d\theta}{dn}$ is set to zero such that at a given instant of time, each axis conforms to an arc. δ is set to $\frac{\pi}{2}$. When the angles of one axis are at their maximum, ($\theta = k\pi$), the angles of the other axis will be zero ($\theta = k\pi + \frac{\pi}{2}$). These two arcs, one at a maximum while the other is at zero, combine to make a single arc incorporating all modules for any value of t. The amplitude parameters, in this case, control the radius of curvature of the arc. As time increases, the arc rolls across the ground, as shown in Fig. 10.

With a non-zero value of $\frac{d\theta}{dn}$, the robot can model the shape of a helix. This configuration can roll while maintaining the helix shape. This motion is used to

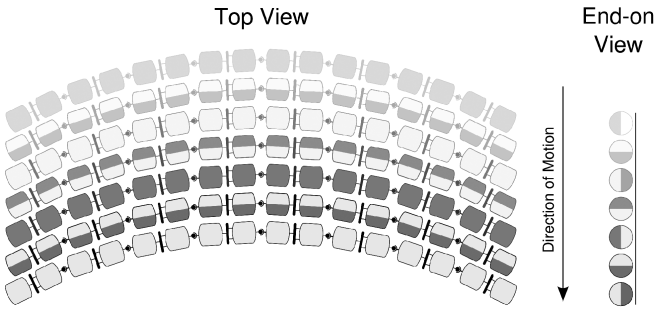

Figure 10. To roll, the snake creates a single arc shape out of its entire length. Although no axial torques can be applied, this arc can rotate around the central axis of the snake. Therefore, if the arc is of a large enough amplitude, it will continually and infinitesimally tip the snake over, causing the robot to roll across the ground.

climb up the outside of poles and the inside of pipes. The width of the helix and the helical pitch angle can be modified with amplitude and $\frac{d\theta}{dn}$. Since this pole-climbing gait is only a small variation of the rolling gait, the robot is capable of smoothly transitioning between rolling on the ground and climbing up a pole.

Although this model only has a handful of parameters, its expressiveness and usefulness is exemplified in the case of climbing a pole. As extraordinary as a pole-climbing robot is, the capability for a smooth transition between ground traversal and crawling up a pole is a novel capability provided for by this simple, yet powerful model of parameterized gaits. This transition does not require any manual positioning of the robot; the operator simply smoothly tightens the snake around a pole by varying a model parameter and the same joint movements that previously rolled the snake robot across the ground now propel it up the pole.

4.2. Scripted Gaits

Many tasks cannot be completed solely by executing a parameterized gait. These cases arise due to task complexity and robot hardware limitations such as size and motor strength. In these cases a scripted gait is used. Unlike parameterized gaits, which are designed to locomote in a wide range of terrains and take variable input parameters to further modify the performance of the gait, scripted gaits are developed specifically for the robot to complete a desired task. Such tasks include stair climbing, gap crossing, reaching into a hole in a wall, railroad track crossing and camera scanning with the head of the robot.

As an example, consider stair climbing. Since none of our existing parameterized gaits are capable of locomoting the robot up and over a significantly sized step, this task requires a series of distinct motions that are designed specifically to for this purpose. To begin this scripted gait, a few modules from the head of the snake are lifted off of the ground. These front modules are then bent to the side such that they rest on top of the next step, as in the left of Fig. 11. Next, the gait undergoes a rolling motion to 'push from below' and 'pull from above' most of the remaining modules onto the top of the step. Once enough of the robots mass is resting on the higher step, a final motion pulls the remaining modules from the bottom of the step to the top (Fig. 11, right).

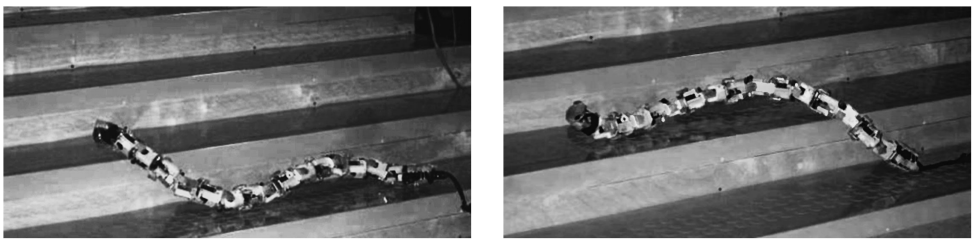

Figure 11. Robot climbing a staircase by lifting the front modules (left), followed by the back modules (right).

Stair climbing requires this seemingly complicated set of maneuvers — perch, roll and pull — because the actuators in the modules have limited strength; in other words, the snake robot is not strong enough to simply reach up and access the next step. Instead, when the robot is perching up, it lifts the modules like a cobra, with each motion maintaining as small a moment arm as possible against the vertical.

Stability is another major constraint of this type of scripted gait. While lifting portions of the robot body off of the ground, the robots center of gravity rises and the robot naturally becomes susceptible to toppling over. Therefore, while perching up, the stair-climbing gait arranges those modules still contacting the ground in a configuration that forms a wide, stable base. While lifting the center modules of the robot to the next step, the side of the step may generate unpredictable forces on the robot; in order to remain stable, modules near the head and tail must be positioned such that the gait is robust to these disturbances.

Unfortunately, stair climbing is a brittle gait. Each of the motions described above, i.e., perching, rolling and pulling, are custom designed for a specific step height. Varying this step height requires the gait to be reprogrammed. This speaks of the advantage of parameterized gaits over scripted graits. With parameterized gaits, varying the gait parameters changes the behavior so that it may adapt to different environments, whereas with scripted gaits, using the gait in an environment that it was not specifically designed for may cause the robot to fail to accomplish its objective. In this instance, programming a new scripted gait is required.

Another example of a scripted gait, which requires stable base forming and reaching against gravity, is gap crossing. Essentially, gap crossing allows the robot to cross over a channel or gap bounded by two parallel walls. Initially, the gait invokes linear progression to drive the robot to the edge of the gap. Once the edge is reached, the robot keeps driving forward over the gap using linear progression. If the gap is narrow enough, the head of the snake robot accesses the other side of the gap and only uses linear progression to cross the channel. So as long as the there is enough mass left on the starting side of the gap and the 'last' module on this side is strong enough to cantilever the forward modules over the channel, then the head of the snake eventually reaches the other side of the gap and can achieve gap crossing using solely linear progression.

Unfortunately, the modules have limited strength and for gaps above a certain width, the robot must invoke a scripted gait to cross the gap. For such cases, the gap-crossing gait starts off with linear progression, but now the 'overhanging' modules over the gap are aimed directly down into the gap. The gait progresses until the length of all of the modules in the gap is slightly larger than the gap itself. At this point, if the last module on the original side of the gap, i.e., the last land-side module, were strong enough, it could simply lift up the overhanging mechanisms to reach across the gap and then invoke linear progression as before. However, this module may not be strong enough to lift all of the modules. Thus, to reduce the burden on this module, the moment arm on the overhanging modules is reduced by bending the middle module of the overhanging modules, forming an 'L' shape. The

last land-side module now lifts the overhanging modules 180°, the middle module unbends and then the last overhanging module rotates by 90°, thereby placing the head of the snake robot on the other side of the gap.

If the gap is too wide, then bending at the half-way point for the overhanging modules is not sufficient because the last land-side module cannot generate enough torque to lift the resulting L-shaped overhanging modules. Instead, the gap-crossing gait forms a 'U' shape overhang bending at the third and second third overhanging modules. To fully reach across the gap, the gait performs similar acrobatics, the whole time trying to keep the moment harm of the modules in the gap as small as possible. With a 16-module snake robot (of length 90 cm), the current gap-crossing gait can traverse a 33-cm gap.

While the scripted gaits are not as elegant as the parameterized ones, sometimes they are necessary. Unfortunately, designing these gaits may require a complicated process. A gait designer must identify a broad 'strategy' for completing the task and then design the series of configurations to reach these goals, while considering motor strength and stability issues.

5. Energetics

Power considerations are important for both development of more efficient gaits and selecting gaits when using the robot in the field. Naturally, we want to optimize power use so as to lengthen the run-time of the robot, whether it be to extend battery life (in a future version of our robot) or minimize heat dissipation. Also, this allows us to maximize performance by using our motors more effectively, which may in turn allow us to design a more lightweight robot. In this section, we report some basic measurements from tests of our core gaits. By using current-sensing chips in the modules to find the current $I(t)$ and knowledge of supply voltage V, we can calculate the power draw $P_i(t) = I_i(t)V$ for each module i in the snake robot. Although we only recieve current readings at discrete times, we can interpolate to generate a continuous $I(t)$ for each module. We then use a suite of in-house tools to create power profiles for different gaits, as well as determine the total power draw for the snake robot in a variety of situations.

5.1. Power Profiles

A power profile is the average power draw during a test run for each module of the robot. We can compute the average power draw $\bar{P}_i$ for any given module i numerically from the instantaneous power draw readings $P_i(t)$ during the test. The power profile is the ordered set of these $\bar{P}_i$ for each module i in the robot.

Typical profiles for gaits we often use are displayed as bar graphs in Fig. 12. All of the experiments in this section were conducted using the most recent generation of our snake robots, using the standard length of 16 modules. These power profiles give constructive information about the gaits, such as which modules draw the most power and, therefore, heat up the fastest, and whether the even and odd modules

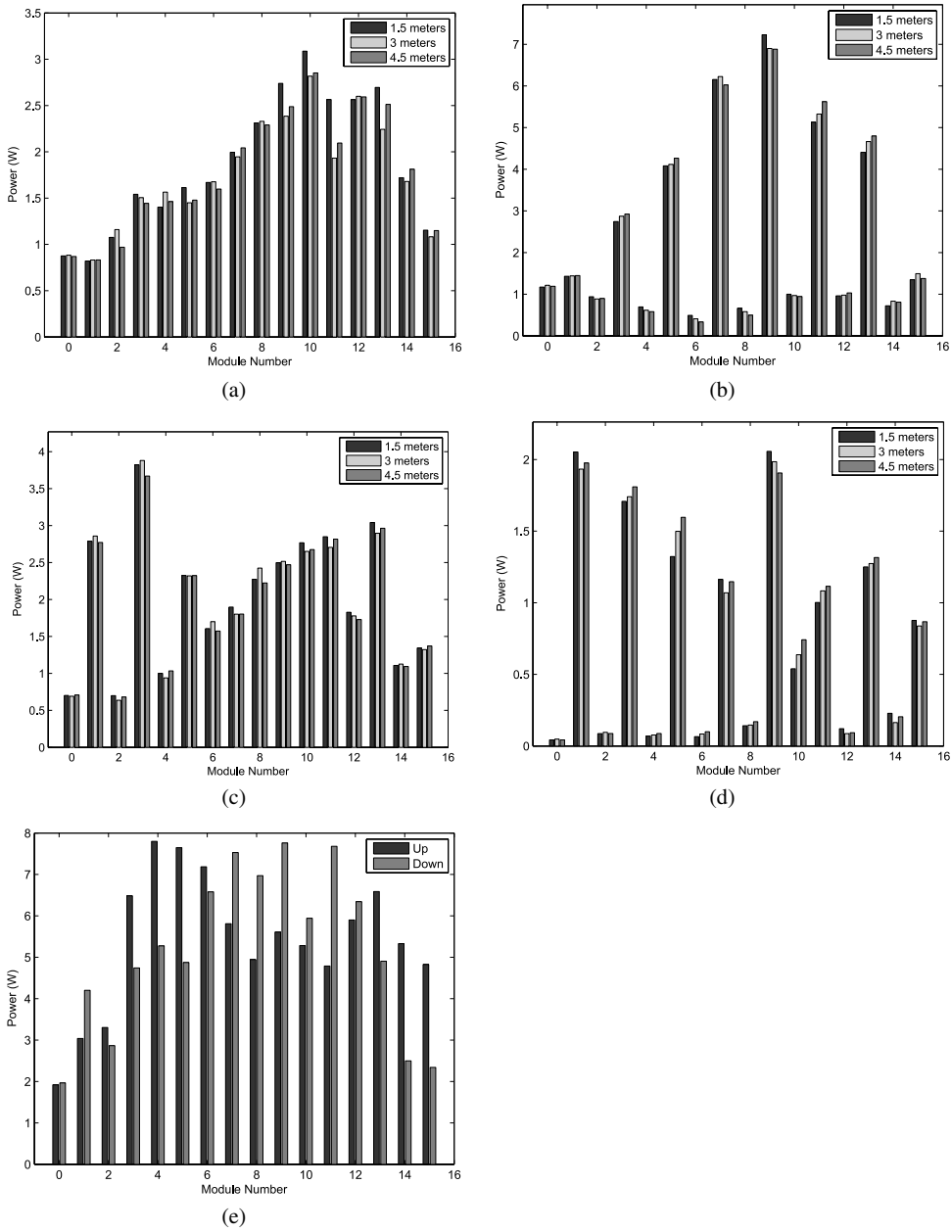

Figure 12. Power profile graphs for a selection of five gaits. These results were averaged from 10 runs of the robot at each distance, for each gait. As expected, the average power draw is independent of distance travelled. (a) Rolling, (b) sidewinding, (c) slithering, (d) linear progression and (e) climbing.

have significantly different power draw magnitudes. The relative magnitudes of the power draw from even and odd modules can even be used to infer whether a gait caused the snake robot to remain upright or to undergo a rolling or tipping motion,

which could be important in choosing a gait to stabilize video from an onboard camera, or in determining stability of a gait. Power profiles also allow us to diagnose problems with individual modules of the snake robot by illustrating when a single module has a large deviation from its expected power use.

- *Rolling*. The rolling gait power profile demonstrates that the center modules use more power than the modules closer to the head and tail, and shows a bias of larger power draw towards the higher numbered modules, located at the tail of the snake robot. This and the fact that the rolling gait is longitudinally symmetric allow us to infer that the weight and drag of the tether and slip ring are significant, causing modules closer to the tail to use more energy.

- *Sidewinding*. When sidewinding, the even modules use more power than the odd modules and there is a natural separation of the power profile into two subprofiles: one made up only of even modules and the other made up only of odd modules. We can infer from this clear dichotomy that the vertical and lateral modules never switch roles and, therefore, the robot does not tip or roll while locomoting. Furthermore, we conclude that the even numbered modules, which use more power, are the modules which lift the snake robot vertically, while the lower energy odd numbered modules form the lateral modules. These odd modules move the elevated portions of the snake robot laterally, with almost no kinetic friction caused by sliding along the ground. Additionally, a bias of power consumption towards the tail of the robot similar to that of the rolling gait can be seen in the vertical modules while sidewinding, matching our conclusion from analysis of the rolling power profile that the significant weight of the tether and slip ring adds to the energy required to lift the tail of the snake.

- *Slithering*. The power profile of the slithering gait shows that even modules, in general, have a higher power draw than odd modules. This indicates that, like the sidewinding gait, the slithering gait maintains an upward orientation. However, the average power draw of the odd numbered modules while slithering is higher than while sidewinding, from which we can infer that there is more kinetic friction encountered by the lateral modules during slithering than sidewinding.

- *Linear progression*. Like the sidewinding and slithering gait, even modules consume significantly more power than odd modules, indicating that the even modules are doing more work and, therefore, are remaining vertical, while the odd modules remain lateral throughout the experiments. Another observation is that the power consumption during linear progression is low compared to both sidewinding and slithering. This is due to the fact that the amplitude of the vertical wave used for linear progression is small in order to improve stability. Due to the wider footprint of slithering and sidewinding, we were able to increase the vertical amplitudes and, therefore, the speed of those gaits. However, to increase the amplitude of the linear progression vertical wave and still maintain

balance and forward motion would require setting the lateral modules to a very wide 'S' shape, which decreases the effectiveness of the gait.

- *Climbing*. The climbing profile corroborates our conclusions drawn from the other gaits. As expected, since the snake robot rotates about the longitudinal axis, there is no distinction between even and odd module power draw. Also matching our previous conclusions, the central modules draw more power.

More generally, we make four conclusions from the data shown in Fig. 12. (i) The modules closest to the center of the snake robot use the most power and, therefore, generate the most heat, in every gait tested. Future work in gait design could use this information to determine where to focus efforts to cool the snake robot or in designing power-sharing pathways for battery power. (ii) The tether causes modules closer to the tail of the snake robot to draw more power than modules near the front; combining these first two effects we get a typical parabolic power profile whose center is shifted slighty towards the rear of the snake. (iii) It is possible to determine whether the robot maintains an upward orientation or rolls around the longitudinal axis by observing only the power draw, which can be important for stabilization of a video feed from an onboard camera or of the snake robot itself. (iv) We can infer from these profiles that the modules composing the vertical wave through the snake robot use more power than those in the lateral wave.

This information can also be used to improve future gait generation efforts. Since we have observed that the vertical modules heat up more rapidly than the lateral modules, we can design gaits that purposefully switch vertical orientation, therefore averaging out the current draw by switching which set of modules are vertical. Also, we can focus development on gaits which depend more on the front and back modules, which may be less effective but will allow the center modules to cool.

5.2. Energy Calculation

Using the power draw for each module $P_i(t)$, as defined before, we can calculate total energy used by the snake robot by integrating the power draw over the length of the experiment and summing the energy use of all the modules. Note that this calculation is based on data from onboard sensors.

In order to select an appropriate gait, one must consider the amount of energy different gaits consume. To this end, experiments were conducted which consisted of marking off intervals of 1.5, 3 and 4.5 m from a starting point on a solid tile floor, and running each core gaits 10 times at each of these distances. The power draw was integrated from the time the robot started moving until it crossed the line signifying the goal. The values of E_{tot} from these experiments are shown in Fig. 13. Included for comparison are data from the snake robot climbing a 11.4-cm diameter pole.

From the data in Fig. 13, we can conclude that sidewinding and rolling, our two lateral locomotion gaits, are the most energy efficient of our core gaits. Rolling composes all of the modules into a small amplitude arc; by minimizing the vertical lifting of modules, rolling is the most efficient of any tested gait.

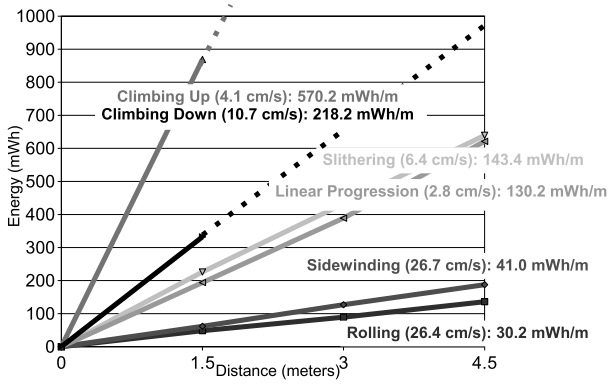

Figure 13. Comparison of energy required to move distances of 1.5, 3 and 4.5 m for three parameterized ground-traversal gaits. Two sets of energy data for a climbing gait, moving 1.5 m upwards and 1.5 m downwards, are also included for comparison, and are extrapolated to 3 and 4.5 m based on the scalability of energy consumption demonstrated by the other gaits.

Inspection of Fig. 13 also shows not only that the best type of lateral locomotion is more efficient than axial locomotion, but shows a distinct clustering of energy use of gaits based on the direction of locomotion. The gaits that moved the snakes laterally both achieved similar results and the gaits that moved the snake forward along its axis also had similar energy consumption properties to each other.

As expected, the climbing gait requires more energy per distance traveled than any of the ground-traversal gaits. Climbing down also requires more energy than any of the ground-traversal gaits. This implies that most of the energy during climbing is actually used to maintain a frictional grip on the pole rather than to locomote the snake robot.

Ideally, these results and conclusions provide insight which enables the creation of more efficient gaits. To this end we conclude some general properties of efficient gaits. (i) They should remain low to the ground. Since we find that gaits that lift modules use more energy, we should minimize the height of modules during locomotion. (ii) Lateral locomotion is more efficient than driving the snake robot in the axial direction. This makes intuitive sense because when the snake robot is straight, small amplitude deviations at any joint result almost purely in lateral motion. Attempting to move purely in the axial direction is similar to trying to move your car sideways; it can be done, but indirectly and inefficiently through a parallel-parking-type manuever.

6. Experiments

In early March of 2006, 2007 and 2008, we evaluated our robots at the Southwest Research Institute (SwRI) in San Antonio, TX, USA. Many robots developed for the US Department of Defense are evaluated at SwRI, which houses a respected robot evaluation test-bed. The six initial tests were crossing a gap, passing through a hole, climbing the inside of a pipe, climbing the outside of a pole, navigating brush and

climbing stairs. In addition to these tests, the robot swam in a pond, traversed along a horizontal pipe, maneuvered through rock and sand, and crawled through a chain-linked fence. In this section, we describe the tasks at SwRI, followed by a discussion on the energetics for these tasks. Although the robots changed between consecutive visits to SwRI, the dimensions, number of modules and overall design principals were the same from year to year; the principal improvements to the design consisted of increasing the robustness of the electronics and torque of the motors.

For normal operation, the robot requires an operator supported by a robot wrangler to manage the tether. The operator control unit (OCU) consists of a laptop computer (Panasonic Toughbook) running software to visualize the robot state, and to command and control the robot. The robot control software is written in C, and is comprised of mathematical functions implementing the gaits and an interface that allows the operator to visualize the gait parameters and to interactively modify gait parameter values. The visualization tool displays information sent to and received from the snake, such as commanded angle, sensor feedback, and temperature and current limits. This visualizer also displays gait parameter values, which could be set by commands from a keyboard or game controller joystick.

6.1. Tasks at SwRI

In 2006, our snake robots were able to cross gaps of varying distances between 7.6 and 22.9 cm. In 2007, the robots were able to cross a gap 30.5 cm wide but was not tested on any larger gaps. In 2008, the new robots were able to traverse a gap of width 40.6 cm. In the most recent results, the robot crossed the gaps with a slight adaptation of the scripted gap-crossing gait described previously.

In 2006 and 2007, the robots were able to pass through 10.2-cm diameter holes, whose centers were located 6.4 cm off of the ground (Fig. 14). These holes opened into varying lengths of PVC tubing, from 2.5 to 30.5 cm. Our robot was able to traverse all of these pipes. Unfortunately, our robot was not able to pass through a hole located 20.3 cm above the ground, but came very close in the SwRI evaluations. The robots were not put through these tests in 2008.

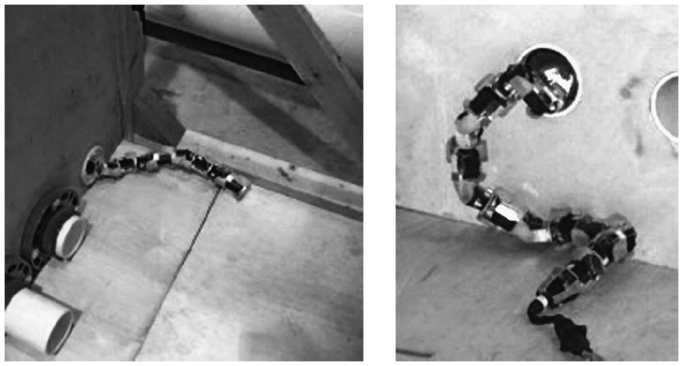

Figure 14. Robot passing through a hole 6.4 cm above the ground (left) and 20.3 cm above the ground (right).

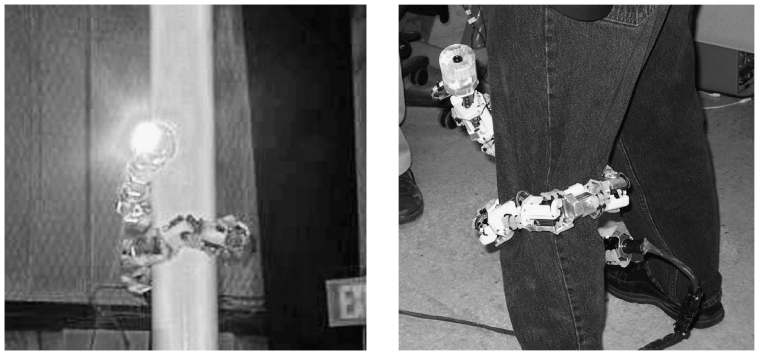

Figure 15. Snake wrapped around a pole and looking around after climbing up (left), and the snake around a volunteer's leg, demonstrating the robot's ability to climb irregular surfaces (right).

In 2006 and 2007, the snake robots were able to climb the inside of a 10.2 cm PVC pipe. In 2006, the robot climbed about 1.6 m in 8 min and 30 s. In 2007, it climbed 4.5 m in 2 min and 34 s. It was also able to climb 4 m in an 20.4-cm diameter pipe in 1 min and 49 s. In 2008, we extended one robot to 24 modules in an attempt to climb the inside of a 30.5-cm diameter pipe; in this configuration, the robot was able to climb 1.3 m in 1 min and 51 s.

Pole climbing, shown in Fig. 15, is perhaps one of the greatest capabilities of the Carnegie Mellon snake robots. At SwRI in 2007, our snake robot traveled across the floor, wrapped itself around the 10.2-cm diameter pole and climbed 5.85 m with the helical pole-climbing gait. The robot completed this sequence in 1 min and 39 s. In addition, the robot climbed with authority and was able to remain stable on the pole while steering the camera module around to look in different directions. To demonstrate the versatility of our climbing gait, we often direct the snake robot to climb volunteers' legs when giving demonstrations.

The robot, encased with a cloth skin, completed the 15-m long brush course in 22 min and 46 s in 2007. For this event, we had one operator selecting gaits to direct the snake robot, and one person who managed the tether and called out simple directions to the operator. Toward the end of the run at 13 min, the motors overheated, so the robot sat still for 2 min to cool. This cool-down period was included in the total time for the run. The robot used a number of gaits, including sidewinding, linear progression and rolling. In the sidewinding gait, much of the robot body lifted above the ground, which appeared inefficient for the terrain. We did not perform this test in 2008 so as to focus on other evaluations.

We designed a gait to climb stairs at Carnegie Mellon, but had to adapt this gait for stair climbing at SwRI because of the different dimensions of their stairs. The 12 rubber covered steps at SwRI had a 12.7-cm rise, 30.5-cm run, were 1.8 m wide and had no barriers on the side. In 2006 and 2007, we were able to climb the stairs, but were not expedient; the best run took 19 min and 40 s. In 2008, with an improved robot and better gait design, the robot was able to climb the stairs in 5 min and 12 s (Fig. 11).

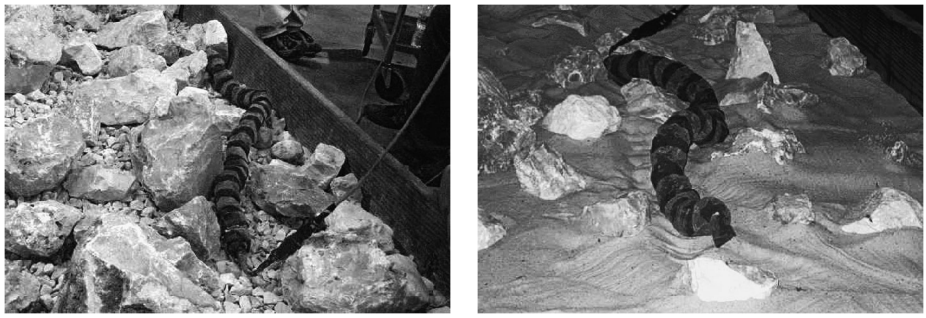

Figure 16. Snake, encased in a protective skin, traversing rocks on gravel (left) and rocks on sand (right).

Traversing large rocks on gravel at SwRI proved to be quite challenging (Fig. 16). In our best run in 2008, the robot traveled 3.3 m in 20 min. This was the first time we attempted this challenge, and perhaps additional study and gait design would increase our performance. Traversing rocks on sand was easier: in 2007, the robot crossed the 4.9-m long course in 10 min and 46 s using a variety of gaits. At the end of the course, a motor amplifier burned out, preventing further progress by the robot. Also, the skin hampered the operator's visibility; because it was hard to determine which side of the robot was up, setting gait parameters became more difficult. We plan to use sensor feedback to alleviate such problems in the future.

In 2007 and 2008, we climbed a Z-pipe which has a horizontal PVC portion, a vertical PVC portion and, again, a final horizontal PVC portion. These sections are connected by a 90° elbow connector, also made of PVC tubing. We attempted this test on a 10.2- and 20.3-cm diameter Z-pipe. In both years, the robot successfully traversed the 10.2-cm diameter pipe fixture. During some runs, the head of the robot briefly was stuck on the lip of the second elbow. After some wriggling, the robot got out of the pipe with some difficulty. We tried several runs on the 20.3-cm diameter Z-pipe but always had trouble negotiating the second elbow connector. Typically, after 2.5 min, one of the modules overheated, causing the experiment to stop (and hence fail).

6.2. Power Usage for SwRI Tasks

We attached the SwRI power logger to the robot, and collected time, voltage and current data. We then analyzed that data to determine power consumption. We observed an average resting load, i.e., power consumption when the robot was stationary, of 9.27 W. We observed a typical power supply voltage between 27.2 and 27.3 V. We studied the power consumption during floor traversal, using the rolling, sidewinding and slithering gaits. We also studied pole climbing for a 10.2-cm diameter PVC pole at 5.1 cm/s, and then at 15.2 cm/s. For both climbs, the evaluation was divided into three segments: climbing up, holding onto the pole and climbing down. Results of these trials are shown in Table 1.

Table 1.
A comparison of power required to locomote and climb at different speeds, taken from a single trial on a pole of diameter 10.2 cm

Event	Mean power (W)	Maximum power (W)	Speed (cm/s)
Floor, rolling gait	48.57	157.03	43.9
Floor, sidewinding gait	53.28	–	29.0
Floor, slithering gait	51.87	–	–
Pole climb up, 5.1 cm/s	99.56	179.91	5.1
Pole hold (from 5.1 cm/s test)	103.46	117.20	5.1
Pole climb down, 5.1 cm/s	76.79	193.13	5.1
Pole climb up, 15.2 cm/s	121.35	222.85	15.2
Pole hold (from 15.2 cm/s test)	113.20	128.31	15.2
Pole climb down, 15.2 cm/s	114.97	223.39	15.2

In terms of speed and holding, we observed that climbing faster uses more power, but consumes less energy per distance traveled: when climbing up, traveling at 15.2 cm/s consumed 22% more power than traveling at 5.1 cm/s. This means that climbing at the higher 15.2 cm/s speed consumed about 60% less energy over the same distance, as compared with climbing at 5.1 cm/s. Likewise, when climbing down, traveling at 15.2 cm/s consumed 50% more power than traveling at 5.1 cm/s, or 50% less energy per unit distance. When holding position on the pole, holding with the parameter settings for travel at 15.2 cm/s consumed 9% more power than holding with the parameter settings for travel at 5.1 cm/s.

We also observed some directional effects while climbing: at a speed of 5.1 cm/s, traveling down consumed 23% less power than traveling up; at a speed of 15.2 cm/s, traveling down consumed 5% less power than traveling up. Finally, we observed that, for both speeds tested, holding position consumed over 90% of the energy used while moving up or down. This information further corroborates our hypothesis, previously mentioned in Section 5, that for both climbing up and climbing down, most of the power used is dedicated to staying on the pole as opposed to moving along it.

The experiments conducted with the test fixtures at the SwRI were useful in externally validating additional results from the Section 5. As reported in the SwRI experiments, the average power used while climbing a 10.2-cm diameter pole at 5.1 cm/s is around 100 W. This compares very reasonably to our onboard power calculations of 80 W while climbing a 11.43-cm diameter tube at 4.0 cm/s. The sidewinding gait consumed 53 W at 29.0 cm/s during the tests at SwRI, compared to 40 W at 26.9 cm/s during laboratory tests. The slithering gait, for which we did not obtain speed information, consumed 52 W during the tests and 33 W in the lab. Finally, the rolling gait consumed 49 W during the SwRI experiments while moving at 43.9 cm/s, while only 29 W in the lab while moving at 25.9 cm/s.

Finally, we should note that energy data at SwRI was measured by recording the current running through the tether to the snake, while the energy data from Sec-

tion 5 was recorded from onboard sensors. This means that the results from the SwRI experiments take into account several factors, such as losses in the tether and onboard power supplies, that are ignored in the data in Section 5. While we realize that makes this an apples-to-oranges comparison, it still provides some intuition on how much power a particular gait consumes because these additional unmodeled power draw terms are approximately constant factors and, therefore, not a factor of which gait is being run. Indeed, each external measurement of power is only 10–20 W higher than internal measurements from a similar test. Therefore, for future work in improving and optimizing gaits, the internal sensor measurements have been shown to be reliable and useful indicators of true power usage of the gait.

7. Conclusions

This paper describes and analyzes a series of gaits for a snake robot comprised of single-d.o.f. modules daisy-chained together, where each axis of rotation is orthogonal to the previous axis. Inspired by biology and based on our empirical experiences with these devices, we have been designing gaits for these robots for several years and have had some impressive demonstrations. In this paper, we describe the insight behind developing these gaits. We have discussed the architecture for this robot elsewhere [2].

We are constantly looking to design new gaits, both parameterized and scripted. Ultimately, we want to improve reliability and robustness. In addition to describing new parameterized gaits, we also seek a more streamlined manner in which we can define scripted gaits. Parameterized gaits are desirable because they are adaptable; for instance, if linear progression is not making sufficient progress due to rough terrain, the operator can easily modify the amplitude of the wave to make the gait more effective. In contrast, if a scripted gait is not effectively performing, the robot operator has no such recourse to adapt the gait to the environment.

We also have characterized power draw information from various gaits. We seek to use this energetics data to guide improvements in the power efficiency of our gaits. Lower power gaits have the added benefit of decreasing the heat generated by our robots, lengthening run times before a pause for cooling is required. In addition, we can compare the performance of our robots to that of actual snakes to gain further insight into biological locomotion.

The next avenue of future research involves using sensor feedback to improve our existing gaits. For instance, sensor feedback could allow the robot to adjust its configuration to prevent tipping while climbing stairs. Through effective use of sensor feedback (touch sensors, accelerometers, current sensing), scripted gaits can be enhanced to better adapt to uncertain environments.

This sensor feedback can also prove useful for parameterized gaits. Currently, when climbing the outside of a pole, the operator tightens the helix radius until the robot gains sufficient traction. Through the use of current and position sensing, the robot itself could determine proper helix pitch and radius to optimally climb a

pole with respect to speed or power efficiency. Furthermore, sensors can be used to enhance the robot with semi-autonomous capabilities, such as maintaining balance and orientation as the operator directs the robot.

In addition to improving the robustness or efficiency of lower level gaits, this sensor feedback could also be used to direct the higher level behavior of the robot. For example, feedback could be used to detect when the robot changes terrain based on a shift in reported power draw and automatically change gaits. A specific case of this would be automatically transitioning from crawling on the ground to wrapping around and climbing to the top of a tree. Combining sensor feedback with velocity estimation would allow for real-time computation of efficiency, enabling the robot to optimize gait parameters to maximize locomotion efficiency, possibly creating new gaits.

References

1. K. Lipkin, I. Brown, A. Peck, H. Choset, J. Rembisz, P. Gianfortoni and A. Naaktgeboren, Differentiable and piecewise differentiable gaits for snake robots, in: *Proc. IEEE/RSJ Int. Conf. on Intelligent Robots and Systems*, San Diego, CA, pp. 1864–1869 (2007).
2. C. Wright, A. Johnson, A. Peck, Z. McCord, A. Naaktgeboren, P. Gianfortoni, M. Gonzalez-Rivero, R. Hatton and H. Choset, Design of a modular snake robot, in: *Proc. IEEE/RSJ Int. Conf. on Intelligent Robots and Systems*, San Diego, CA, pp. 2609–2614 (2007).
3. N. Vidal and S. B. Hedges, Molecular evidence for a terrestrial origin of snakes, *Proc. Roy. Soc. B: Biol. Sci.* **271**, S226–S229 (2004).
4. G. S. Chirikjian and J. W. Burdick, A modal approach to hyper-redundant manipulator kinematics, *IEEE Trans. Robotics Automat.* **10**, 343–354 (1994).
5. G. S. Chirikjian and J. W. Burdick, Kinematically optimal hyper-redundant manipulator configurations, *IEEE Trans. Robotics Automat.* **11**, 794–806 (1995).
6. J. R. L. Elwood and D. Cundall, Morphology and behavior of the feeding apparatus in *Cryptobranchus alleganiensis* (Amphibia: Caudata), *J. Morphology* **220**, 47–70 (1994).
7. C. Gans, *Biomechanics: An Approach to Vertebrate Biology*. University of Michigan Press, Ann Arbor, MI (1980).
8. R. E. Chodrow and C. R. Taylor, Energetic cost of limbless locomotion in snakes, *Fed. Proc.* **32** 422 (1973).
9. M. Walton, B. C. Jayne and A. F. Bennett, The energetic cost of limbless locomotion, *Science* **249**, 524–527 (1990).
10. A. Bennett, S. Secor and B. Jayne, Locomotor performance and energetic cost of sidewinding by the snake *Crotalus cerastes*, *J. Exp. Biol.* **163**, 1–14 (1992).
11. H. Ikeda and N. Takanashi, Joint assembly movable like a human arm, *US Patent 4,683,406* (1987).
12. E. Palug, T. Ohm and S. Hyathi, The JPL serpentine robot: a 12 DOF system for inspection, in: *Proc. IEEE Conf. on Robotics Automation*, Nagoya, pp. 3143–3148 (1995).
13. M. A. Hannan and I. D. Walker, Kinematics and the implementation of an elephant's trunk manipulator and other continuum style robots (http://www.ces.clemson.edu/~ianw/Hannan_Walker_JRS.pdf), *J. Robotic Syst.* **20**, 45–63 (2003).
14. A. Wolf, H. B. Brown, R. Casciola, A. Costa, M. Schwerin, E. Shamas and H. Choset, A mobile hyper redundant mechanism for search and rescue tasks, in: *Proc. IEEE Conf. on Robot and Intelligent Systems*, Las Vegas, NV, pp. 2889–2895 (2003).

15. G. Granosik and J. Borensteain, Integrated joint actuator for serpentine robots, *IEEE/ASME Trans. Mechatronics* **10**, 473–481 (2005).
16. T. Takayama and S. Hirose, Development of Souryu I&II, *J. Robotics Mechatron.* **15**, 61–69 (2003).
17. S. Hirose, *Biologically Inspired Robots: Snake-Like Locomotors and Manipulators*. Oxford University Press, Oxford (1993).
18. G. Miller, http://www.snakerobots.com/index.html
19. M. Yim, S. Homans and K. Roufas, Climbing with snake-like robots, in: *Proc. IFAC Workshop on Mobile Robot Technology*, Jejudo Island (2001).
20. J. Ostrowski and J. Burdick, The geometric mechanics of undulatory robotic locomotion, *Int. J. Robotics Res.* **17**, 683–702 (1998).
21. Y. Umetani and S. Hirose, Biomechanical study of serpentine locomotion, in: *Proc. 1st RoManSy Symp.*, Udine, Italy, pp. 171–184 (1974).
22. M. Yim, Locomotion gaits with polypod, in: *Video Proc. IEEE Int. Conf. on Robotics and Automation*, San Diego, CA (1994).
23. F. Barazandeh, B. Bahr and A. Moradi, How self-locking reduces actuator torque in climbing snake robots, in: *Proc. IEEE Int. Conf. on Advanced Intelligent Mechatronics*, Zurich (2007).
24. J. Gonzalez-Gomez, H. Zhang, E. Boemo and J. Zhang, Locomotion capabilities of a modular robot with eight pitch–yaw-connecting modules, in: *Proc. 9th Int. Conf. on Climbing and Walking Robots*, Zurich (2006).
25. J. Gonzalez-Gomez, H. Zhang and E. Boemo, Locomotion principles of 1D topology pitch and pitch–yaw-connecting modular robots, in: *Bioinspiration and Robotics: Walking and Climbing Robots*. Advanced Robotics Systems International and I-Tech Education and Publishing, Vienna (2007).
26. W.-M. Shen, M. Krivokon, H. Chiu, J. Everist, M. Rubenstein and J. Venkatesh, Multimode locomotion *via* SuperBot reconfigurable robots, *Auton. Robots* **20**, 165–177 (2006).

About the Authors

Matthew Tesch graduated from Franklin W. Olin College of Engineering with a BS in Engineering, with a concentration in systems, in 2007. After graduation, he began Graduate School at the Robotics Institute of Carnegie Mellon University. He is currently completing his second year of PhD work under his advisor, Howie Choset.

Kevin Lipkin is completing an integrated program at Carnegie Mellon University, expecting to graduate with a BS in Mechanical Engineering and an MBA from the Tepper School of Business. He has worked in Howie Choset's Biorobotics Lab for several years during his undergraduate career and is currently transitioning to a position at Red Zone Robotics.

Isaac Brown received a BS from Carnegie Mellon University with minors in Robotics and Creative Writting, in 2008. While there, he spent 2.5 years doing snake robotics research at Howie Choset's Biorobotics Lab, which included publishing and presenting a paper at IROS 2007. He now resides in California, where he works in the Measurement, Integration and Test Section of the Jet Propulsion Laboratory.

Ross L. Hatton received a SB in Mechanical Engineering from the Massachusetts Institute of Technology in 2005 and a MS in the same from Carnegie Mellon University in 2007. He is currently a PhD student in Robotics and Mechanical Engineering at Carnegie Mellon University. His research focuses on understanding the fundamental mechanics of locomotion and on finding abstractions that facilitate human control of unconventional locomotors.

Aaron Peck received his BS at Carnegie Mellon University in Mechanical Engineering, with a minor in Robotics and Fine Art. During his undergraduate career, he worked in Howie Choset's Biorobotics Lab for 2 years. He is currently working for WET Design as a Product Engineer designing water feature technology.

Justine Rembisz completed her undergraduate degree at Carnegie Mellon University in Mechanical Engineering. During her time at Carnegie Mellon University she worked in both the Nanorobotics Lab and the Biorobotics Lab. Her interests are in soft robotics and mechatronic design. She currently works as a researcher at iRobot Corporation.

Howie Choset is an Associate Professor of Robotics at Carnegie Mellon University, where he conducts research in path planning, motion planning, estimation, mechanism design and hybrid controls. Much of this work has two foci: snake robots for search and rescue, manufacturing and medical robotics, and coverage for de-mining and autobody painting. He directs the Undergraduate Robotics Minor at Carnegie Mellon University and teaches an overview course on Robotics which uses series of custom developed Lego Labs to complement the course work. His students have won Best Paper awards at the RIA in 1999 and ICRA in 2003, he has been nominated for Best Papers at ICRA in 1997 and IROS in 2003 and 2007, and won Best Paper at IEEE Bio Rob in 2006. In 2002 the MIT Technology Review elected him as one of its top 100 innovators in the world under 35. In 2005, MIT Press published a textbook, lead authored by him, entitled *Principles of Robot Motion*.